Werk

Jahr: 1986
Kollektion: fid.geo
Signatur: 8 Z NAT 2148:59
Digitalisiert: Niedersächsische Staats- und Universitätsbibliothek Göttingen
Werk Id: PPN1015067948_0059
PURL: http://resolver.sub.uni-goettingen.de/purl?PPN1015067948_0059

LOG Id: LOG_0043
LOG Titel: Magnetostratigraphy of Neogene equatorial Pacific pelagic sediments
LOG Typ: article

Übergeordnetes Werk

Werk Id: PPN1015067948
PURL: http://resolver.sub.uni-goettingen.de/purl?PPN1015067948
OPAC: http://opac.sub.uni-goettingen.de/DB=1/PPN?PPN=1015067948

Contact

Niedersächsische Staats- und Universitätsbibliothek Göttingen
Georg-August-Universität Göttingen
Platz der Göttinger Sieben 1
37073 Göttingen
Germany
Email: gdz@sub.uni-goettingen.de

J Geophys (1986) 59:183–194

Journal of Geophysics

Magnetostratigraphy of Neogene equatorial Pacific pelagic sediments

Norbert Weinreich [1, 3] **and Fritz Theyer** [2]

[1] Institut für Geophysik, Ruhr-Universität Bochum, Postfach 102148, 4630 Bochum 1, Federal Republic of Germany
[2] Department of Geological Science, University of Southern California, University Park, Los Angeles, CA 90089, USA

Abstract. The magnetostratigraphic record of lower Miocene to Quaternary sediments cored in the central equatorial Pacific is presented in this study. The VLHPC (variable length hydraulic piston corer) recovered Neogene deposits at the DSDP (Deep Sea Drilling Project) Leg 85 sites 573, 574 and 575, which are relatively uniform siliceous-calcareous oozes. The basis for all paleomagnetic analyses are the progressive alternating demagnetization experiments of each sample. The results constitute the first opportunity to elaborate a magnetostratigraphic record down to the lower Miocene in this area. In various sections biostratigraphic age control was applied to calibrate the measured paleomagnetic polarity patterns to the geomagnetic timescale. The systematic increase of accumulation/time downhole at each site, as well as the systematic decrease of deposition on the profile from south (site 573) to north (site 575), reflects the northward motion of the Pacific plate underneath the equatorial Pacific stationary zone of high biogenic mass-production. The generally constant morphology of its northern flank for the last 20 million years is documented by the paleomagnetic results.

Key words: Paleomagnetism – Magnetol – biostratigraphy – Equatorial Pacific – Sedimentation rates

Introduction

Repeatedly, the central Pacific was the destination of cruises of the DSDP (Deep Sea Drilling Project) Legs 5, 8, 9 and 16, recovering several hundreds of metres of sediment with the conventional 'rotary' technique (McManus et al., 1970; Tracey et al., 1971; Hays et al., 1972; van Andel et al., 1973). The focal point of all investigations was to obtain almost complete biostratigraphies and to study the geologic evolution and paleo-oceanography of this region during the Cenozoic (Berger, 1973; Winterer, 1973; van Andel et al., 1975).

The prominent geological structure in this area is a tight equator-parallel zone of extremely high accumulation of predominantly calcareous microfossils which extend from about 4°S to 5°N and is believed to be about constant at least for the Neogene (van Andel et al., 1975). With increasing latitude the composition of sediments changes gradually and then more rapidly from a dominant calcareous to a more siliceous one. In principle, the lateral Pacific plate motion relative to this belt of high bio-productivity provides, together with the abnormal deep-reaching calcium compensation depth, CCD (Berger, 1970), the characteristic lithostratigraphic composition of the central equatorial Pacific deposits.

Despite the relatively frequent work on conventional piston cores (Hays et al., 1969; Opdyke et al., 1974; Theyer and Hammond, 1974; Theyer et al., 1978), most were located more to the west, the central equatorial Pacific having yielded rather meagre paleomagnetic results in the past. This was generally due to the limitation given by the maximum length of traditional piston cores and to the very weak intensities of the natural remanent magnetization, NRM, of the highly calcareous sediments. Therefore, the use of the VLHPC technique provides the first opportunity of establishing more extensive magnetostratigraphic reference profiles in this region for much of the Neogene.

At sites 573 to 575, which form a south-north transect parallel to 134° of western longitude across the northern flank of the equatorial sediment bulk (Fig. 1), the paleomagnetic studies cover the Quaternary and Pliocene and parts of the Miocene. Measurable NRM intensities were observed only throughout sections with predominant siliceous composition. The more calcareous deposits, in general, provided no interpretable results.

The down-hole patterns of the magnetic reversals are correlated to the geomagnetic polarity time-scale of Berggren et al., (1986) in this study. For some of the Miocene sections biostratigraphic criteria had to be employed in places to calibrate the identified polarity transitions which are separated from the younger continuous sequences either by the lack of sampling or by prominent hiatuses found in the sedimentary column (Baron et al., 1985). The magnetostratigraphic data are then used to calculate apparent rates of sedimentation. Their systematic variations with age and latitude, in turn, are interpreted as the response of Pacific plate motion and constant biogenic mass-production during the Neogene.

Materials and methods

The sampling broadly followed age versus depth relations based on the biostratigraphic record. The intervals typically represent a resolution in time on the order of 10^4 years.

3 *Present address:* De-Vries-Hof 9, D-3000 Hannover 61, Federal Republic of Germany

Offprint requests to: N. Weinreich

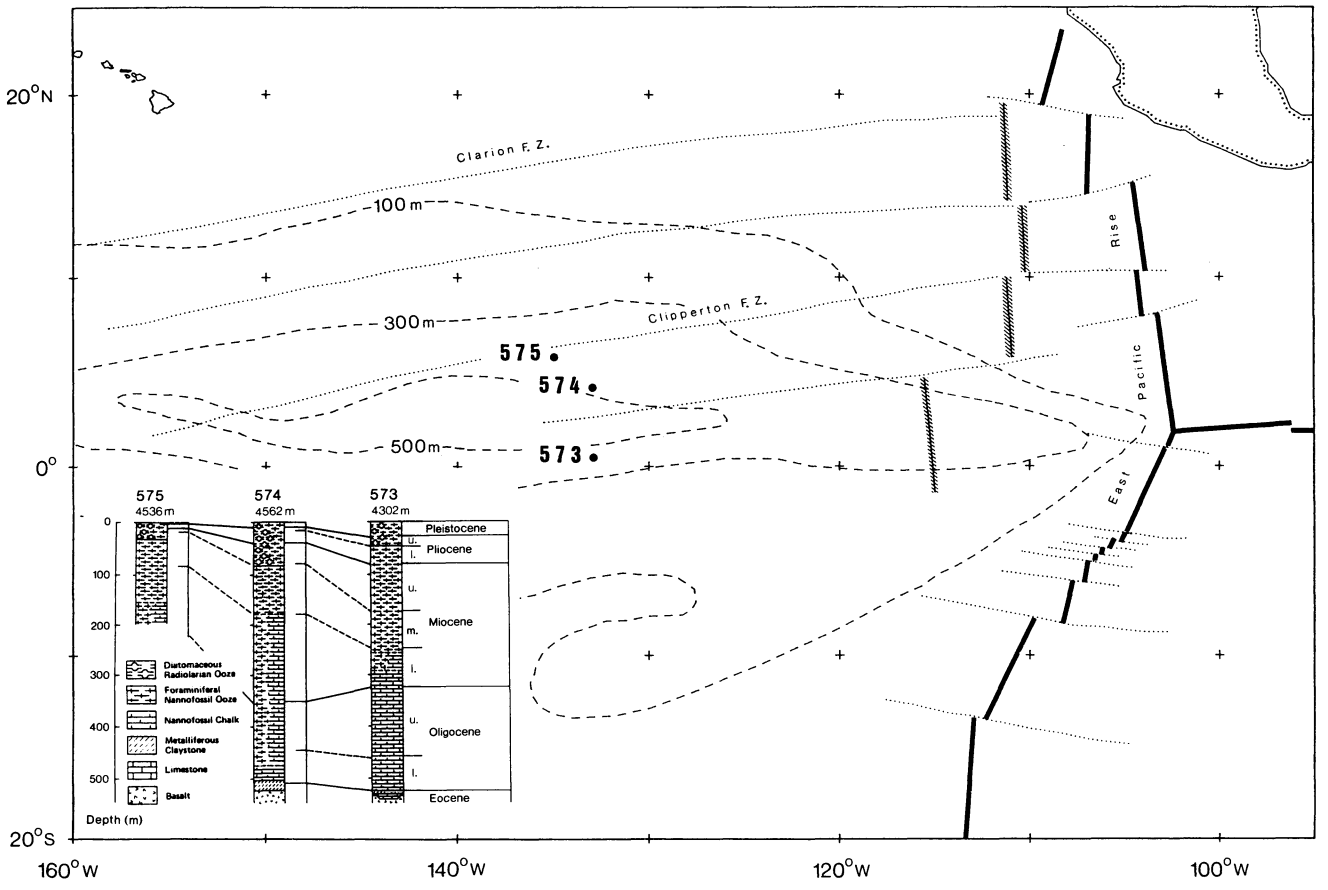

Fig. 1. Location map of DSDP Leg 85 sites 573, 574 and 575 in the central equatorial Pacific. Isochrons of the sediment thickness are marked by *dashed lines*. *Dotted lines* indicate fracture zones (F.Z.), *heavy black lines* the East-Pacific-Rise and the Galapagos Rise, *hatches* the fossil 'Mathematicians-Ridge'. The *insert* shows the lithostratigraphy, the biostratigraphic ages and the depth below sea-level

For the present study, all measurements were made on triaxial cryogenic magnetometers.

In addition to the NRM measurements, systematic stepwise alternating-field, AF, demagnetization series were applied to each sample using a Schonstedt GSD-1 single-axis demagnetizer. These series were taken mostly to the 50 mT level in steps of either 2.5 mT or 5 mT. Then the direction of the stable remanence was determined for each sample individually by analyses of different graphic representations of the demagnetization data. For this purpose the NRM-normalized intensity of magnetization versus the applied demagnetization field, vetor diagrams (Zijderveld, 1967) and stereographic projections of the total vectors and difference vectors (Hoffman and Day, 1978) were analysed. After this, a stable remanence direction for each sample was defined by the mean of measured directions during at least three consecutive demagnetization steps which showed the least directional scatter.

Because of the low, near-equatorial latitudes of the Leg 85 sites, the measured inclination data show mostly scatter of a few degrees about zero. Therefore, 180° changes in the stable declination data were used to define polarity transitions of the Earth's magnetic paleofield, which makes the determination of true polarity of the samples difficult in the absence of an absolute azimuthal orientation. Coring related variations in the declination data, in addition, give a complex polarity signal (Weinreich and Theyer, 1985). The declinations used for the magnetostratigraphic analyses are corrected by means of their respective stable core-mean values to, on average, 0° or 180° for either normal or reverse paleofield polarity (Weinreich and Theyer, 1985). For the Neogene, the series of the Earth's magnetic polarity patterns are specified to the traditional nomenclature of McDougall (1977), using the numerical ages of Berggren et al. (1986).

Results

Before discussing the results there will be a brief review of typical examples of the paleomagnetic response of different sediments to successive AF demagnetization. At the same time, this will allow a general outline of their magnetization characteristics and illustrate the paleomagnetic methods used in this study. The examples of demagnetization response discussed below are typical for the recovered siliceous-calcareous biogenic oozes essentially deposited during the Neogene in the central equatorial Pacific.

Figure 2 shows a typical Type I demagnization behaviour (Tauxe et al., 1984; Bleil, 1986). As illustrated here, most of all Type I samples show a monotonous decrease in remanent magnetization upon progressive AF demagnetization (Fig. 2a). The vector diagrams (Fig. 2b), whose orthogonal components decrease continuously towards the origin of the coordinate system in both the horizontal and vertical plane, prove the above interpretation. The total vectors of remanence as well as the difference vectors form

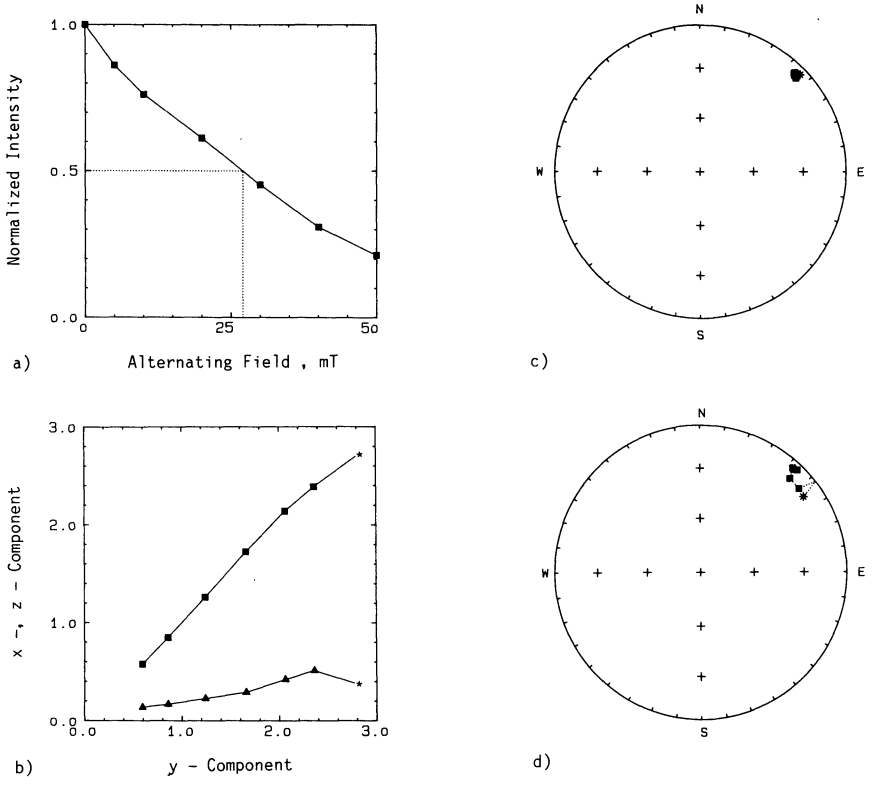

Fig. 2a–d. Type I demagnetization characteristics of the remanence.
a Demagnetization curve: variation of the NRM-normalized remanent intensity of the magnetization as a function of the maximum alternating-field amplitude. The *dotted line* indicates the mean destructive field.
b Vector diagrams: variation of the orthogonal components of the remanence (in 10^{-3} A/m) in the *x,y* plane (*squares*) and the *y,z* plane (*triangles*). The *asterisks* indicate the NRM values. The sequence of demagnetization steps follow those in **a**.
c Stereographic projection of the total vectors of the remanence. The *asterisk* indicates the NRM direction.
d Stereographic projection of the difference vectors of the remanence. The *asterisk* indicates the first demagnetization interval. On the stereographic projections *closed symbols* mark positive, *open symbols* negative inclinations. Subsequent demagnetization steps are connected by great circles

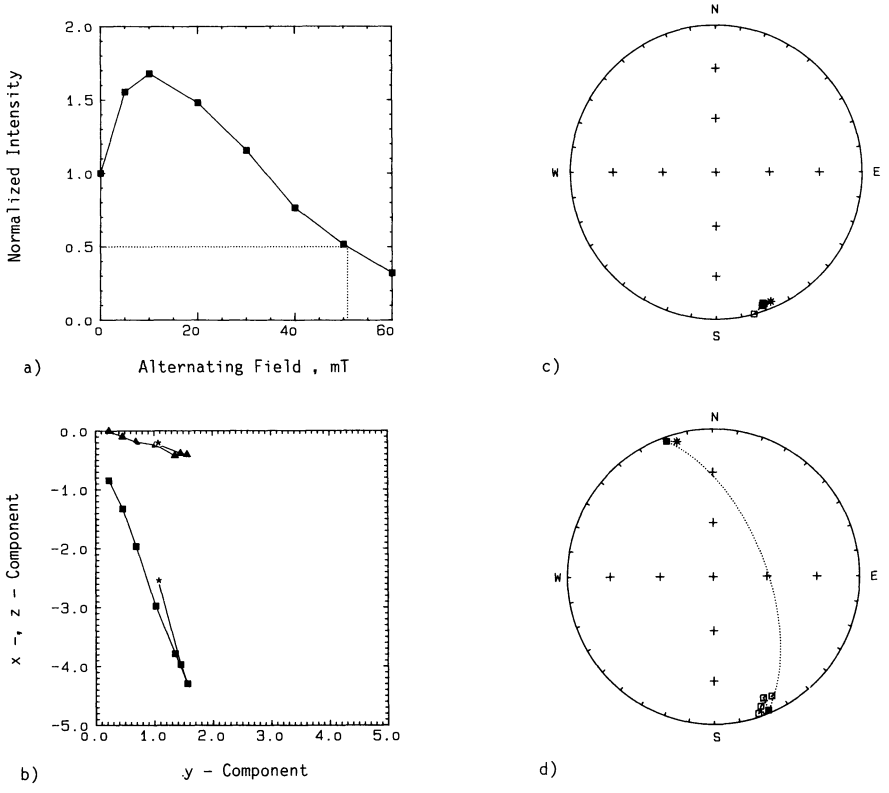

Fig. 3a–d. Type II demagnetization characteristics of the remanence (see Fig. 2)

a very close cluster in the stereographic projections round the same directional mean (Fig. 2c and d). This confirms an essential single-component stable remanence.

In clear contrast, Fig. 3 illustrates a Type II demagnetization response of a multi-component system with almost antiparallel directions of remanence. This is demonstrated by the increase of the NRM-normalized magnetization upon progressive demagnetization followed by a continuous decrease (Fig. 3a). After the destruction of a predominant less stable component, causing the observed increase of the remanent total intensity by the vectorial superposition of two antiparallel-directed components, the stable one

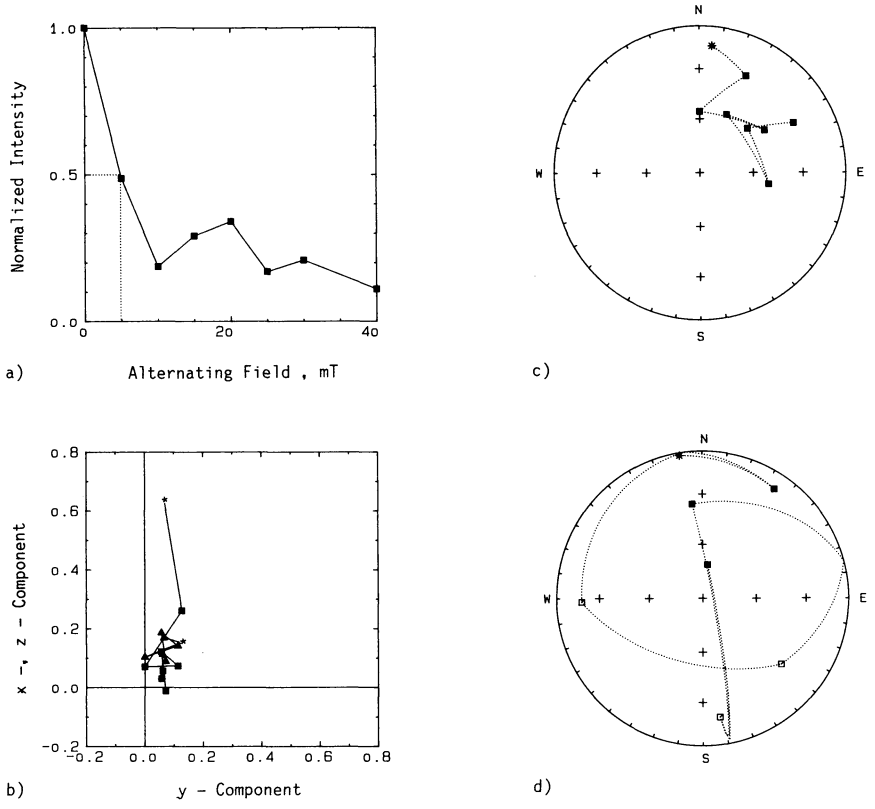

Fig. 4a–d. Type III demagnetization characteristics of the remanence (see Fig. 2)

dominates exclusively. This interpretation is supported by the increase of the orthogonal components in the vector diagrams which turns to a decrease towards the origin (Fig. 3b). Even though the stereographic projection of the total vector of magnetization (Fig. 3c) shows only one direction, the difference-vector diagram (Fig. 3d) allows a qualitative and quantitative definition of two roughly antiparallel directions. Here the magnetically less stable fraction of remanence is interpreted as a viscous magnetic overprint during the present normal geomagnetic Brunhes Epoch.

Finally, Fig. 4 gives an example of the demagnetization response labelled as Type III. Although apparently stable in direction, as one might infer from the stereographic projection of the total vectors (Fig. 4c), the other diagrams point to the erratic behaviour upon AF treatment (Fig. 4). These features have been observed as dominant throughout the highly calcareous sediments which, in turn, have very low NRM intensities.

In the graphic representations of the demagnetization behaviour discussed, the declination data have already been corrected as previously described. The very detailed AF demagnetization and interpretation of the demagnetization features of each sample is of essential advantage at low latitudes. It became obvious that the directional information of a Type I magnetization can be correlated to a normal polarity and a Type II one to a reverse polarity of the magnetic paleofield configuration, respectively. Independent of the lithofacies of the sediment sequences recovered, the remanence carried by the magnetic grain fraction deposited during the Neogene in the central equatorial Pacific is, in general, highly accepted as opposed to viscous overprinting during the normal magnetic paleofield configuration of the Brunhes Epoch. This causes the Type II characteristics of those samples deposited during reverse paleomagnetic field configurations. Therefore, with the classification of the demagnetization behaviour of remanent magnetism used in this study, an additional relevant criterion is available to unequivocally define the exact magnetic polarity of the magnetization so analysed.

Magnetostratigraphies

The declination/inclination logs (Figs. 5, 6 and 9) elaborated from the analyses discussed above provide the basis for the magnetostratigraphic interpretation that follows. The individual polarity sequence at each bore-hole is in general correlated to the geomagnetic time-scale assuming that the topmost continuous polarity indicates the Brunhes normal Epoch and the first 180° shift of the stable declination defines the Brunhes/Matuyama boundary at 0.73 my. The magnetic data from subsequent cores were stratigraphically compiled assuming that 180° changes between cores were not indicative of polarity transitions but, rather, results of rotations of the cores themselves. In any case, this method was guided by the demagnetization classification and by the inclination where possible and, in addition, aided by biostratigraphic criteria.

Site 573

Site 573 is the southernmost of the three-site SN transect along about 134°W, which cuts across the northern flank of the equatorial Pacific high-productivity belt (Fig. 1). A drastic decrease in the NRM intensity at about 45 m downhole, exceeding one order of magnitude, defines the limit of the paleomagnetically interpretable data. This gradient coincides with the lithologic change from cyclic siliceous-calcareous oozes to entirely calcareous oozes, documented by a significant colour change (Mayer and Theyer et al., 1985). The NRM intensities throughout this lithologic unit

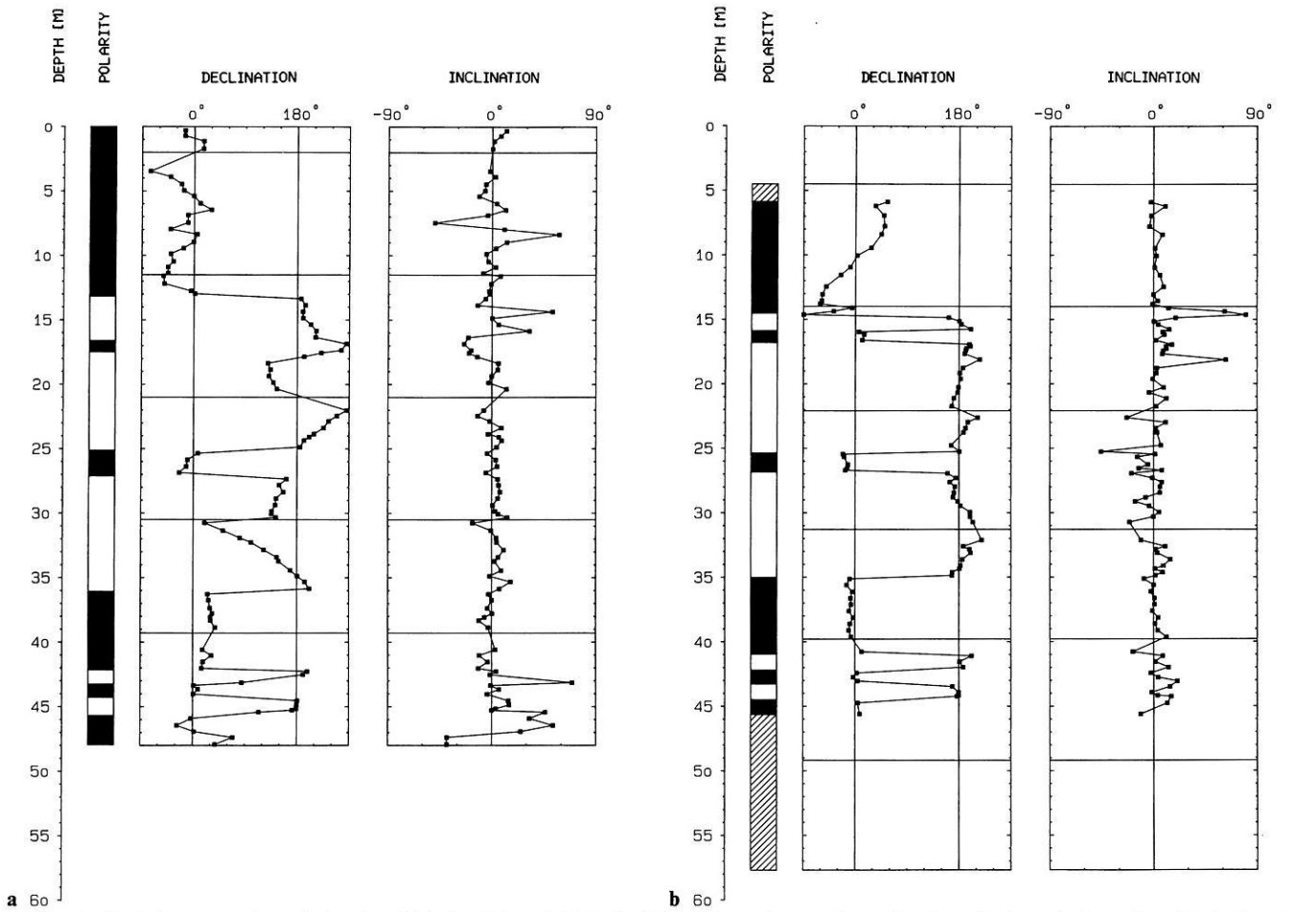

Fig. 5a, b. Paleomagnetic polarity for (**a**) hole 573 and (**b**) hole 573A. The columns show the down-hole variation of stable inclination and corrected declination (see text) and paleomagnetic polarity. *Black* indicates intervals of normal polarity; *white*, intervals of reversed polarity; and *striping*, intervals that could not be interpreted

vary about a mean of $(1.41 \pm 0.82 \times 10^{-3}$ A/m, similar to other Neogene siliceous-calcareous marine sediments (Kent and Spariosu, 1983; Tauxe et al., 1984; Bleil, 1986).

The down-hole polarity pattern derived from the stable declination data (Fig. 5) and their magnetostratigraphic correlation is shown in Fig. 11. At this site all polarity changes were found within cores and the interpretation of either normal or reverse polarity is proved by the variation between Type I and Type II magnetization characteristics.

As the topmost sediments represent the radiolarian *Buccinosphaera invaginata* zone (Riedel and Sanfilippo, 1978) defined by the First Appearance Datum, FAD, of this species, they can be dated younger than 0.23 my (Johnson and Knoll, 1975; Nigrini, 1985). This result agrees well with the nannofossil CN15 zone (Bukry, 1975; Pujos, 1985), therefore, defining the uppermost sequence of uniform declination clearly as of Brunhes age. The directional change further down in the two holes (Fig. 5) are interpreted as the Brunhes/Matuyama boundary at 0.73 my. In the cored sections below, the down-hole pattern in the declinations yield an unequivocal reversal stratigraphy for the last 3.3 my. A more or less constant rate of sedimentation was calculated, from the age versus depth relation of Fig. 11, to be 14.2 ± 0.2 m/my throughout the Plio-/Pleistocene with a small amount of variation down-hole at both parallel holes. This calculation is based on the linear interpolation between magnetostratigraphic fixpoints.

Site 574

At site 574, located near the northern edge of the equatorial Pacific high-productivity belt, throughout the upper Miocene to Quaternary sections of cyclic siliceous-calcareous oozes, a mean NRM intensity of $(1.8 \pm 1.2) \times 10^{-3}$ A/m was measured. Due to the limitations imposed by these sediments, polarity sequences could be derived from the stable declinations down-hole only for the upper 50 m sub-bottom and a short interval between 76 m and 84 m sub-bottom (Fig. 6).

The uppermost core at hole 574 shows one uniform polarity sequence which can be interpreted as being of Brunhes age, proved by the positive stable inclination data (Fig. 6). Biostratigraphically, these sediments are dated to late Pleistocene as indicated by the distinguished nannofossil CN14/CN15 zones (Bukry, 1975; Pujos, 1985). The coincidence with the nannofossil FAD of *Gephyrocapsa caribbeanica* in the topmost deposits of core 574-2 dates its top older than the geomagnetic Jaramillo Event within the reversed Matuyama Epoch (Barron et al., 1985). Below, the next interval of normal polarity, as defined by the stable inclinations and Type I characteristics of remanence, indicates the Olduvai Event; the Brunhes/Matuyama boundary and the Jaramillo Event are missing in this hole. This gap is probably caused by lost sediments during coring. Because of mechanic deformations within core 574-3, the polarity

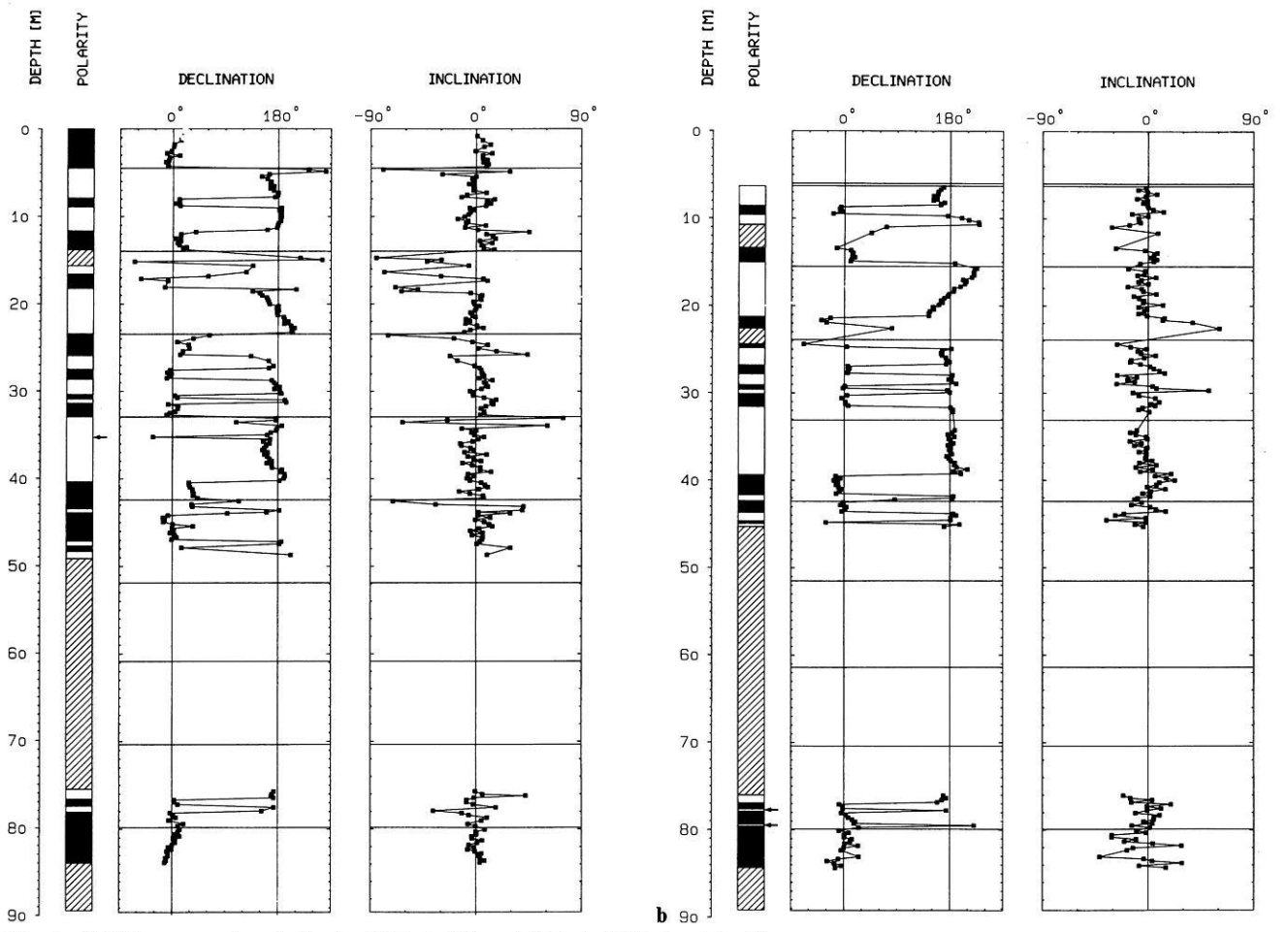

Fig. 6a, b. Paleomagnetic polarity for (**a**) hole 574 and (**b**) hole 574A (see Fig. 5)

pattern of the geomagnetic Gauss Epoch can only partially be identified. The four normal events within the reversed Gilbert Epoch can easily be identified (Fig. 11). The transitions in core 574-5/6 define the geomagnetic Epoch 5. Furher below, a brief normal event occurs which had not been known in any magnetostratigraphy (Opdyke et al., 1974; Theyer and Hammond, 1974; Theyer et al., 1978) or in the geomagnetic time-scales based on marine magnetic anomalies (Berggren et al., 1986).

In hole 574A, a similar situation to the one in hole 574 occurs (Figs. 6 and 11). Core 574A-2 correlates with the reversed Matuyama Epoch based on the stable inclinations and the Type II demagnetization characteristics. Then the first interval of normal polarity was interpreted as the Olduvai Event, biostratigraphically proved by the nannofossil LAD *Coccolithus pelagicus* (Pujos, 1985). The following polarity sequence, in parts, is incomplete throughout this hole because of disturbed sediments (Fig. 6). The complete polarity pattern of the geomagnetic Gilbert Epoch and Epoch 5 can be distinguished at hole 574A, as well as the short interval of normal polarity below Epoch 5. It is identified at the same stratigraphic level as in hole 574. Therefore, this interval can be assumed to be real.

The apparent rates of sedimentation vary about a factor of two throughout the last 6 my. They increase from 5.3 ± 0.2 during the geomagnetic Brunhes to Gauss Epochs to 11.1 ± 0.1 m/my during the Gilbert Epoch and Epoch 5.

In the two parallel holes 574 and 574A between 76 m and 84 m sub-bottom, paleomagnetic unequivocally interpretable data could be obtained (Fig. 6). Intervals of normal and reverse polarity were derived from the change between Type I and Type II demagnetization characteristics of remanence. The magnetostratigraphic interpretation of this interval is based on the results of biostratigraphy. Figure 7 shows the zonations of the four dominant groups of planctonic microfossils throughout the sedimentary column. In the tropical Pacific, the foraminifera zones N14 and N16 as well as the nannofossil zones CN7 and CN6 are characteristic of the geomagnetic Epoch 11 (Berggren and Van Couvering, 1974). The radiolarian species *Diartus petterssoni* is also usually correlated to Epoch 11 (Theyer and Hammond, 1974; Theyer et al., 1978). The transition of diatom species *Actinocyclus moronensis/Coscinodiscus yabei* is dated to 11.3 my (Burckle, 1978) and, therefore, falls within this geomagnetic epoch. For this sub-bottom interval, the biostratigraphically derived rate of sedimentation was calculated to be about 24 m/my (Barron et al., 1985). Referring to this relation, the paleomagnetically studied sequence of 8.3 m length should cover about 0.35 my (Fig. 11). Considering that geomagnetic Epoch 11 consists of two intervals of normal paleofield configurations (Berggren et al., 1986), the derived polarity pattern has to be correlated to one of these intervals. Two biostratigraphic data can be identified within this sediment sequence: the transition of nannofossil zones CN6/CN7, dated to 12 my (Bukry, 1975; Pujos, 1985), and the above-mentioned dia-

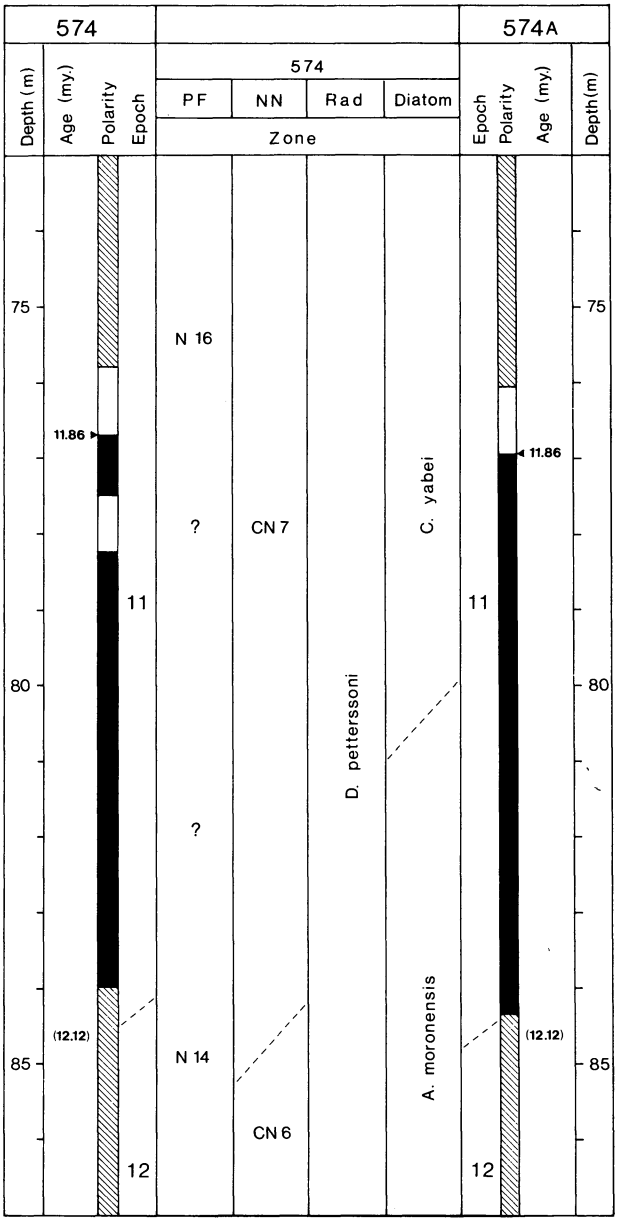

Fig. 7. Magneto- and biostratigraphy throughout the upper Miocene sediments at hole 574 and 574A. The foraminifera zones (*PF*) follow those given by Berggren (1969), nannofossil zones (*NN*) from Bukry (1975), radiolarian zones (Rad) from Riedel and Sanfilippo (1978) and diatom zones from Burckle (1972). *Black intervals* indicate normal, *white intervals* reversed polarity of the Earth's magnetic paleofield. Throughout the *hatched intervals* no data are available or the paleomagnetic measurements do not provide unequivocally interpretable results. The numbers are ages in my

tom transition *A. moronensis/C. yabei*. In addition, the entire interval belongs to the radiolarian zone *D. petterssoni* (Nigrini, 1985) which is usually dated from 12.6 and 11.1 my. According to the biostratigraphic data, it is obvious to correlate this specific interval of normal polarity to the oldest sequence of normal paleofield configuration within Epoch 11 (Fig. 11).

Site 575

Site 575 constitutes the endpoint of the SN transect across the equatorial Pacific high-productivity zone (Fig. 1). At this site Miocene to Quaternary sediments were recovered. The NRM intensities throughout the cyclic siliceous-calcareous oozes, which gradually change to pale brown oozes, are similar to those previously discussed. A mean of $(2.1 \times 1.2) \times 10^{-3}$ A/m was measured.

A magnetostratigraphy from Quaternary into the lower Miocene was established (Fig. 11), unfortunately with some upper and middle Miocene gaps due to prominent hiatuses (Barron et al., 1985). The radiolarian zone *B. invaginata* and the nannofossil zone CN16 prove that the topmost sediments in the two parallel holes 575 and 575C were deposited during the Brunhes Epoch (Pujos, 1985; LaBracherie, 1985). Below, in the sequence, follow the Matuyama and Gauss Epochs as documented by the declination data (Fig. 8) and the demagnetization characteristics. The latter defines the actual paleofield polarity easily (Fig. 11). The Gauss/Gilbert boundary at 3.4 my is immediately followed by the Gilbert/Epoch 5 boundary at 5.35 my. This is in agreement with the biostratigraphy (Barron et al., 1985), substantiating the fact that the entire sequence of the Gilbert normal events is missing due to a late Miocene hiatus (Barron et al., 1985). Hole 575C bottoms with its second core at about 6.4 my defined by the magnetostratigraphy (Fig. 11).

The paleomagnetic sequence throughout hole 575, in parts, provides a poor magnetic record masking the magnetostratigraphic information of Epochs 6 to 8 (Fig. 8). The simultaneous FAD of the two diatom species *Thalassiosira burckliana* and *C. yabei* at the same stratigraphic level (Barron, 1985) is caused by a prominent hiatus covering the entire geomagnetic Epoch 9. This interpretation is proved by other planctonic microfossils (Fig. 9). Within a short interval the two radiolarian data FAD *Didymocyrtis antepenultimus* and FAD *D. petterssoni*, both dated to about 9.5 my (Theyer and Hammond, 1974), and the radiolarian FAD *Diartus hughesi*, dated to 11.5 my (Theyer et al., 1978; Nigrini, 1985), are observed in the tropical Pacific. According to this biostratigraphic record throughout cores 575-3/4 (Fig. 9), the magnetostratigraphic interpretation of the polarity record derived from the declination log and the demagnetization behaviour of remanence covers geomagnetic Epochs 11 to 14 (Fig. 11). The magnetostratigraphic age of bottom of core 575-4, the deepest one studied at this hole, is about 13.5 my which agrees well with the biostratigraphy. Differences between both datings may result from deformed sediments as well as from the solution affecting the calcareous microfossils (Pujos, 1985). Due to the disturbed sediments at hole 575B, cored parallel to holes 575 and 575C, the magnetostratigraphic results are poor and not discussed in detail here. Nevertheless, they are shown on the appropriate Figs. 8 and 11. The apparent rates of sedimentation which are calculated from the magnetostratigraphy at holes 575 and 575C are listed in Table 1.

In Fig. 8 the hole 575A inclination/declination logs are shown and the elaborated polarity pattern opposed against the biostratigraphic results in Fig. 10. The coincidence of the nannofossil zone CN2 and the foraminifera zone N6 with the geomagnetic Epoch 17 verify the results of previously published analyses (Ryan et al., 1974; Berggren and Van Couvering, 1974). Hence, the radiolarian datum FAD *Stichocorys wolffii* dated to 17.6 my (Nigrini, 1985) appears to be too young according to the magnetostratigraphy. The poorly defined transition between the diatom species *Triceratum pileus* and *Denticulopsis nicobarica* is usually observed

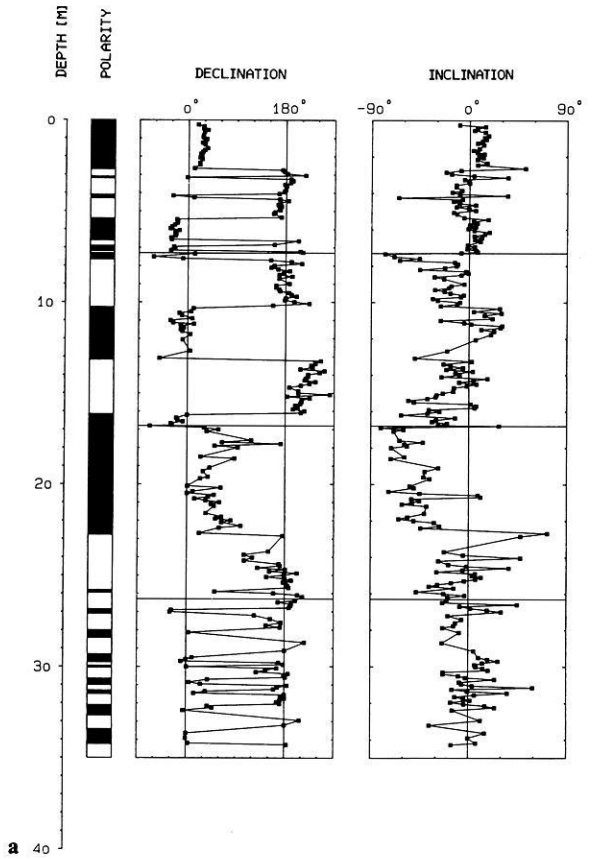

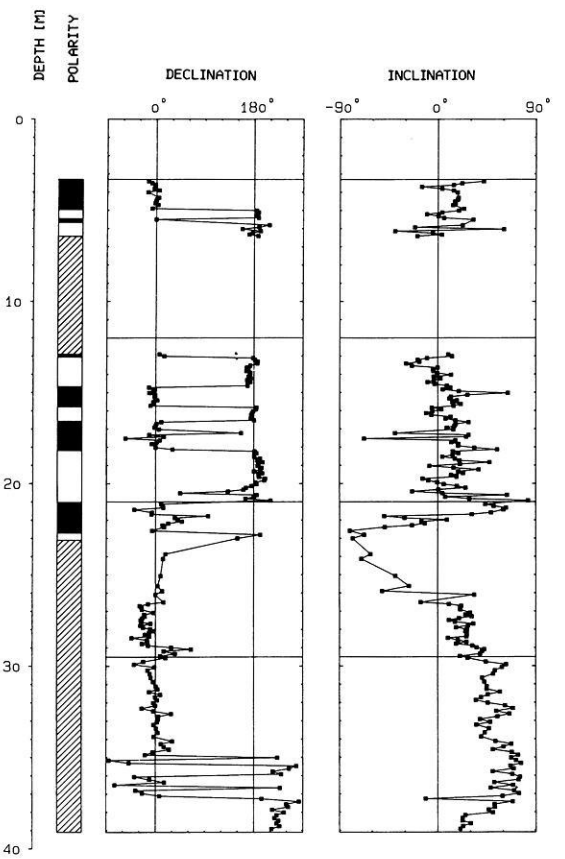

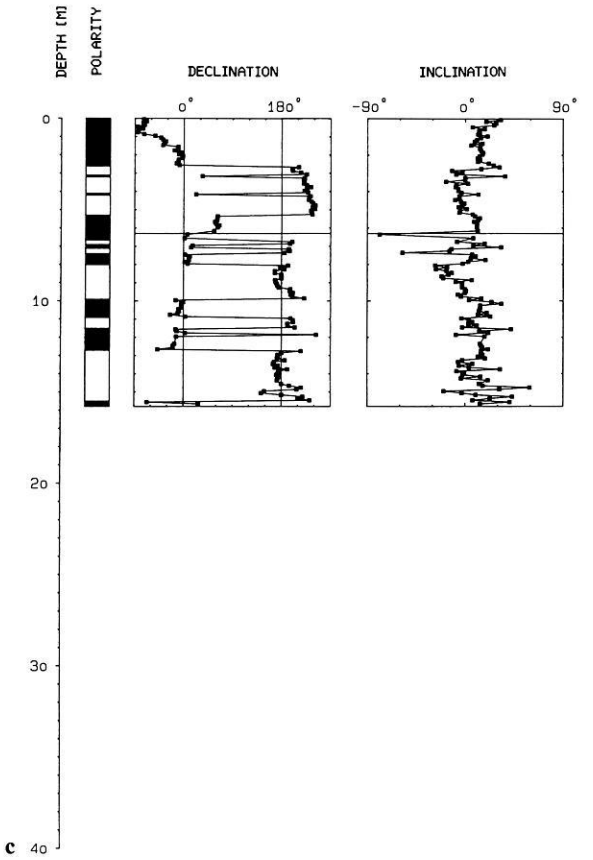

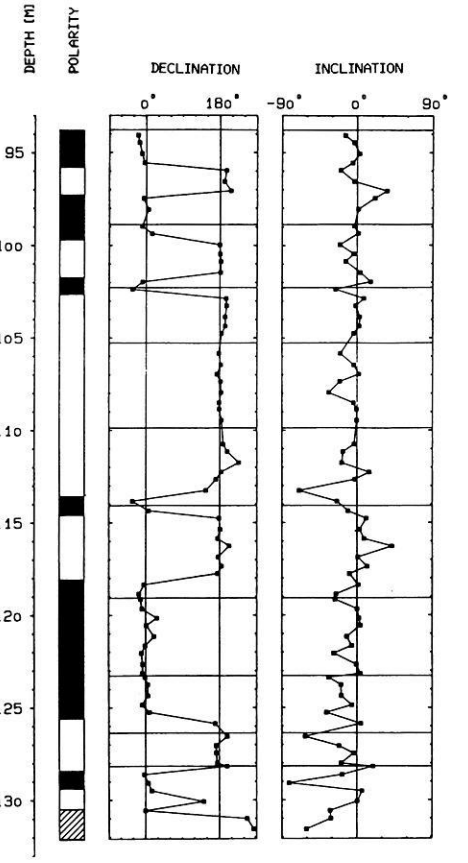

Fig. 8a–d. Paleomagnetic polarity for (**a**) hole 575, (**b**) hole 575B, (**c**) hole 575C and (**d**) hole 575a (see Fig. 5)

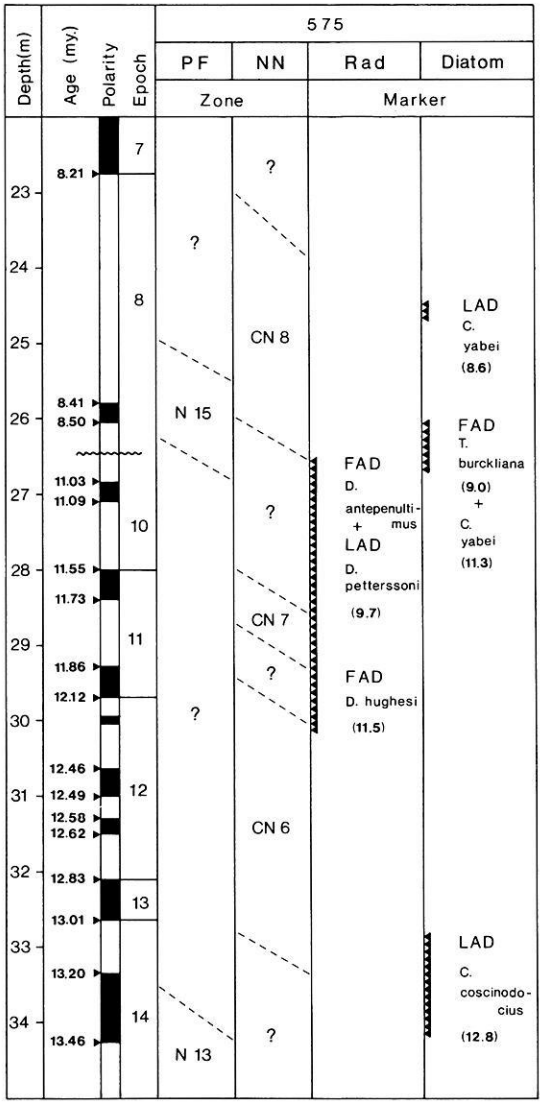

Fig. 9. Magneto- and biostratigraphy throughout the upper Miocene sediments at hole 575 (see Fig. 7)

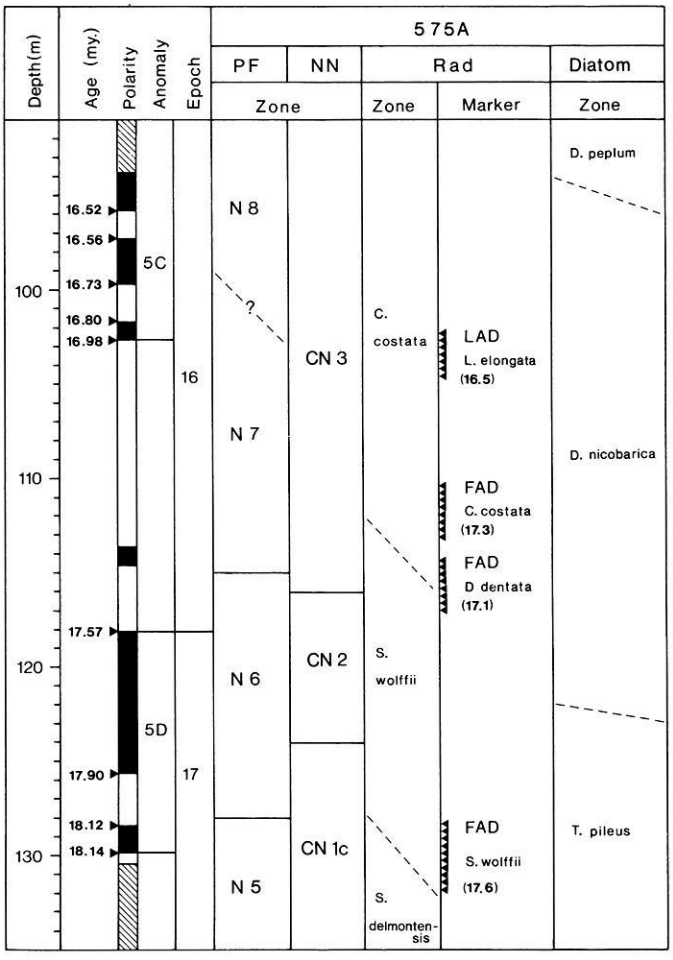

Fig. 10. Magneto- and biostratigraphy throughout the lower Miocene sediments at hole 575A. The marine magnetic anomalies are numbered after LaBrecque et al. (1977) (see Fig. 7)

in the younger sequence of Epoch 17 (Burckle, 1978; Barron, 1985). The geomagnetic Epoch 17/16 boundary mostly coincides with the radiolarian FADs *Dorcadospyris dentata* and *Calocyletta costata*, dated to 17.3–17.1 my (Theyer and Hammond, 1974; Nigrini, 1985). The geomagnetic Epoch 16 is characterised by the following bio-horizons: nannofossil zone CN3, foraminifera zone N7, radiolarian zone *C. costata* and diatom zone *D. nicobarica* (Berggren, 1969; Bukry, 1975; Barron, 1985). The transition of diatom zones *D. nicobarica*/*Cescinodiscus peplum* can be distinguished together with the youngest interval of normal polarity within geomagnetic Epoch 16, as demonstrated in Fig. 10 (Burckle, 1978; Barron, 1985). This gives sufficient agreement of Miocene magneto- and biostratigraphies throughout the sedimentary column at hole 575A and in comparison to the literature.

From the magnetostratigraphically derived age versus depth relation at hole 575A, an apparent rate of deposition of about 21.1 m/my can be calculated. In comparison to the younger rates, a systematic increase of sediment accumulation can be observed with increasing depth at this site.

Table 1. Variation of apparent rates of sedimentation at sites 573, 574 and 575 with age and plate-tectonically reconstructed paleogeographic latitudes

Site No.	Age range (my)	Latitude range	Apparent rate of sedimentation (m/my)
573	0 – 3.3	*0.5°N*–0.4°S	14.2±0.2
574	0 – 3.4	*4.2°N*–3.2°N	5.3±0.2
	3.4– 6.0	3.2°N–2.4°N	11.1±0.1
	11.8–12.1	0.7°N–0.5°N	24
575	0 – 3.5	*5.9°N*–4.8°N	2.3±0.1
	5.1– 8.8	4.3°N–3.2°N	5.6±0.2
	10.5–13.5	2.7°N–1.8°N	3.1
	16.5–18.1	0.9°N–0.5°N	21.1

The present-day geographic site-latitude is underlined

This behaviour is very unsual for marine sediments, due to the continuously increasing compaction with depth. At 114 m sub-bottom an additional interval of normal polarity occurs within geomagnetic Epoch 16, which is not known in the literature and, therefore, can not be correlated to the geomagnetic time-scale. Assuming a constant rate of deposition, this event lasts about 50 ky.

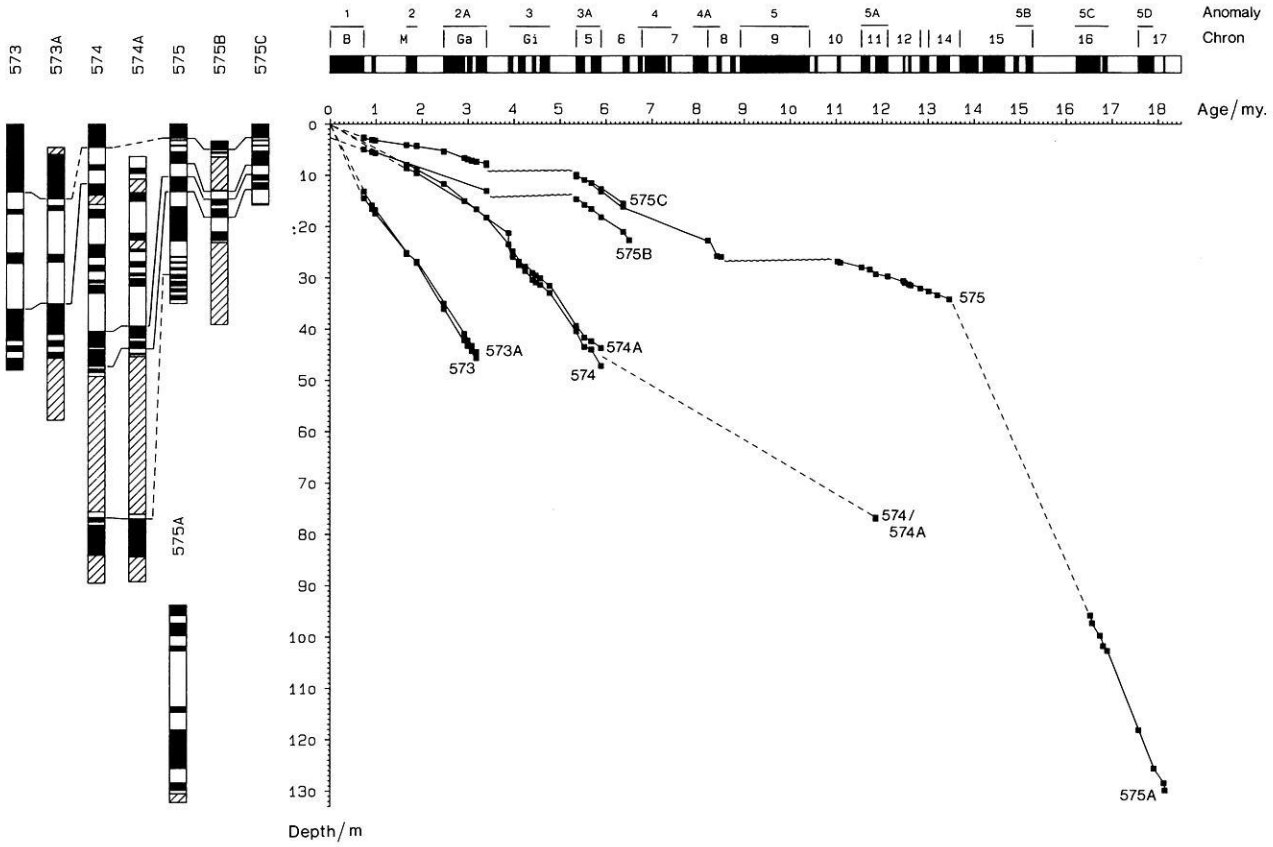

Fig. 11. Summary of the magnetostratigraphies at site 573, 574 and 575. The paleomagnetically derived polarity patterns are correlated to the geomagnetic polarity time-scale of Berggren et al. (1986). *Black intervals* indicate normal, *white intervals* reversed polarity of the Earth's magnetic paleofield. Throughout the *hatched intervals* no data are available or the paleomagnetic measurements do not provide unequivocally interpretable results. *Arrows* indicate polarity intervals identified by one datapoint and in one hole only. *Wavy lines* mark hiatuses

Regional magnetostratigraphic synthesis

Figure 11 summarizes the magnetostratigraphies of all discussed sediment sequences at sites 573 to 575 (Fig. 1). The age versus depth relations show an obvious increase with age and a systematic decrease with progressive northward distance from the equator. These results are quantified in Table 1. For various time intervals the range of paleolatitude, where the deposition took place, and the corresponding rates are listed. The separation is based on significant changes in the rate of sedimentation and/or is oriented due to gaps of information. The latitudinal range derived by the paleo-tectonical reconstructions is calculated from a northward drift of the Pacific plate during the Neogene of about 0.3°/my (Epp, 1978; 1984; Weinreich, 1985).

It becomes obvious that, independent of the appropriate age, the sediments are deposited at comparable paleolatitudes at about the same rates. The sedimentation rate of 21.1 m/my of lower Miocene deposits at site 575 accumulated at 0.4°N–0.9°N correlates according to size with 24 m/my for the upper Miocene at site 574 accumulated at 0.5°N–0.7°N. Almost identical rates can be observed for the upper Miocene at site 575 and the Plio-Pleistocene sediments at site 574, both deposited at identical paleolatitudes (Table 1). In Fig. 12 the apparent rates of sedimentation are plotted as a function of the plate-tectonically reconstructed paleogeographic latitudes. From south to north, first, an increase can be observed, followed by a continous decrease of sedimentation. The interval between 13.5–10.5 my at site 575 (Table 1) disagrees with this unequivocal trend. Here, an extremely high solution of the biogenic carbonate (Pujos, 1985) causes the obvious difference between the calculated *apparent rate of sedimentation and their actual* accumulation. In this context it has to be considered that almost similar paleolatitudes do not correspond to the same age. Therefore, time-dependent variations in the paleogeographic regime, e.g. changes in depth of the CCD, influence carbonate solution.

The variation of accumulation rates, derived from magnetostratigraphies (Fig. 11) depending on different geological ages and paleogeographic latitudes, is the result of two superposed effects: the northward motion of the Pacific plate and the paleogeographically fixed position of the equatorial high-productivity belt of biogenic deposits. After van Andel et al. (1975), the NS extension of this structure and the general behaviour of deposition can be assumed to be constant at least during the Neogene. Therefore, the increase of accumulation with depth at sites 574 and 575 cannot be interpreted as the time-dependent variation of sedimentation at the present-day drillsite location. Rather, they reflect the northward drift of the paleo-sedimentation floor underneath the zone of extreme, but constant, gradients of sediment accumulation. This interpretation explains the distinguished differences of sedimentation rates and, therefore, describes the geographic structure of the equatorial sediment bulk since the Miocene (Fig. 12). The

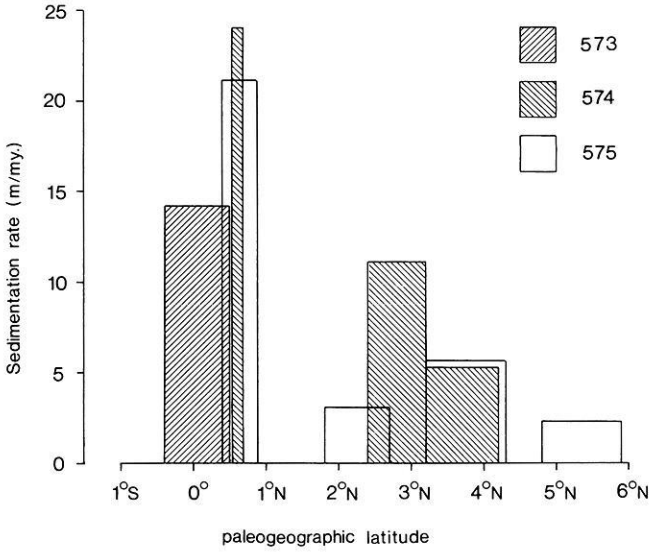

Fig. 12. Variation of the apparent rates of sedimentation as a function of the plate-tectonically reconstructed paleomagnetic latitude

latitudinal range represented by the oldest sediments at sites 574 and 575 define the maximum of sedimentation of microfossil skeletons a little north of the equator. The Plio-/Pleistocene deposits at site 573 were accumulated at latitudes south of this maximum (Fig. 12). To the north, the sedimentation decreases to less than 25% of its maximum. The low rate of 2.3 m/my observed for the Plio-/Pleistocene sediments at site 575 represent the northern edge of the equatorial sediment bulk (Fig. 1). Figure 12 can be interpreted as an image of the equatorial sediment bulk paleotopography during the last 20 my, which implies that any changes in the paleoceanographic regime or prominent geological events like the closing of the central American Isthmus did not affect its sedimentary conditions.

This discussed model of the paleogeographic structure of the equatorial Pacific extreme biogenic mass-production, based on the magnetostratigraphic record of deep-sea cores, corroborates and quantifies the results of previous studies in this area. Those results locate the maximum of deposition at about 1° north of the equator with an extension to about 5°N. Now, this statement could first be conspicuously verified by magnetostratigraphic investigations. Finally, the results prove the assumed northward drift of the Pacific plate of 0.3°/my during the Neogene.

Acknowledgements. We would like to thank all our ship-board colleagues of DSDP Leg 85 for their friendly co-operation. Special thanks are due to Prof. Bleil and V. Spieß for their discussion and valuable comments. J. Barron and C. Nigrini kindly assisted with their stratigraphic data.

The financial support of N.W.'s research by the Deutsche Forschungsgemeinschaft is gratefully acknowledged. F.T.'s research was in part supported under National Science Foundation grants OCE78-000 and OCE82-00000.

References

Barron, J.A.: Late Eocene to Holocene biostratigraphy of the equatorial Pacific Ocean, DSDP Leg 85. In: Initial reports of the Deep Sea Drilling Project **85,** Mayer, L., Theyer, F., et al., pp. 413–456. Washington: U.S. Government Printing Office 1985

Barron, J.A., Nigrini, C.A., Pujos, A., Saito, T., Theyer, F., Thomas, E., Weinreich, N.: Synthesis of central equatorial Pacific DSDP Leg 85 biostratigraphy: refinement of Oligocene to Quaternary biochronology. In: Initial reports of the Deep Sea Drilling Project, vol. **85**, Mayer, L., Theyer, F., et al., pp. 905–934. Washington: U.S. Government Printing Office 1985

Berger, W.H.: Planctonic foraminifera: selective solution and the lysocline. Marine Geology **8**, 111–138, 1970

Berger, W.H.: Cenozoic sedimentation in the eastern tropical Pacific. Geol. Soc. Am. Bull. **84,** 1941–1954, 1973

Berggren, W.A.: Paleogene biostratigraphy and planctonic foraminifera of northern Europe. In: Leiden, Proc. First Internat. Conf. Planctonic Microfossils, Bronnimann, P., Renz, H.H., eds. 121–160, 1969

Berggren, W.A., Van Couvering, J.A.: The late Neogene: biostratigraphy, geochronology, and paleoclimatology of the last 15 million years in marine and continental sediments. Palaeogeography, Palaeoclimatology, Palaeoecology **16,** 1–126, 1974

Berggren, W.A., Kent, D.V., Flynn, J.J.: Paleogene geochronology and chronostratigraphy. In: Geochronology and the geological record, Snelling, N.J., ed.: London, Geol. Soc. London, Spec. paper, 1986 (in press)

Bleil, U.: The magnetostratigraphy of NW Pacific sediments, DSDP Leg 86, In: Initial reports of the Deep Sea Drilling Project **86,** Heath, G.R., Burckle, L.H., et. al.: Washington: U.S. Government Printing Office 1986 (in press)

Bukry, D.: Coccolith and silicoflagellate stratigraphy, north-western Pacific. In: Initial reports of the Deep Sea Drilling Project vol. 32, Larson, R.L., Moberly, R., et al., pp. 677–701. Washington: US Government Printing Office 1975

Burckle, L.H.: Late Cenozoic planctonic diatom zones from the eastern equatorial Pacific. Nova Hedwigia **39,** 217–246, 1972

Burckle, L.H.: Early Miocene to Pliocene diatom levels for the equatorial Pacific. Geol. Res. Devel. Cent. Indonesia, Spec. Publ. **1,** 25–44, 1978

Epp, D.: Age and relationships among volcanic chains on the Pacific plate. Ph.D. thesis, University of Hawaii, 1978

Epp, D.: Possible perturbations to hotspot traces and implications for the origin and structure of the Line Islands. J. Geophys. Res. **89,** 273–287, 1984

Hays, J.D., Saito, T., Opdyke, N.D., Burckle, L.H.: Pliocene-Pleistocene sediments of the eastern equatorial Pacific: their paleomagnetic, biostratigraphic, and climatic record. Geol. Soc. Am. Bull. **80,** 1481–1514, 1969

Hays, J.D., et al.: Initial reports of the Deep Sea Drilling Project, vol. **9**. Washington: US Government Printing Office 1972

Hoffman, K.A., Day, R.: Separation of multi-component NRM: a general method. Earth Planet. Sci. Lett. **40:** 422–438, 1978

Johnson, D.A., Knoll, A.H.: Absolute ages of Quaternary radiolarian datum levels in the equatorial Pacific. Quaternary Res. **5,** 99–110, 1975

Kent, D.V., Spariosu, D.J.: High-resolution magnetostratigraphy of Caribbean Plio-Pleistocene deep-sea sediments. Palaeogeography, Palaeoclimatology, Palaeoecology **42,** 46–64, 1983

LaBracherie, M.: Quaternary radiolarians from the equatorial Pacific, DSDP Leg 85. In: Initial reports of the Deep Sea Drilling Project vol. **85**, Mayer, L., Theyer, F., et al., pp. 499–510. Washington: US Government Printing Office 1985

LaBrecque, J.L., Kent, D.V., Cande, S.C.: Revised magnetic polarity time scale for the late Cretaceous and Cenozoic time. Geology **5,** 330–335, 1977

Mayer, L., Theyer, F., et al.: Initial reports of the Deep Sea Drilling Project **85**. Washington: U.S. Government Printing Office 1985

McDougall, I.: The present status of the geomagnetic polarity time scale. Research School of Earth Sciences, A.N.U., Publ. No. 1288, 1977

McManus, D.A., et al.: Initial reports of the Deep Sea Drilling Project, vol. **5**. Washington: US Government Printing Office 1970

Nigrini, C.A.: Radiolarian biostratigraphy in the central equatorial

Pacific. In: Initial reports of the Deep Sea Drilling Project, vol. **85**, Mayer, L., Theyer, F., et al., pp. 511–552. Washington: US Government Printing Office 1985

Opdyke, N.D., Burckle, L.H., Todd, A.: The extension of the magnetic time scale in sediments of the central Pacific ocean. Earth Planet. Sci. Lett. **22,** 300–306, 1974

Pujos, A.: Cenozoic nannofossils, central equatorial Pacific, DSDP Leg 85. In: Initial reports of the Deep Sea Drilling Project, vol. **85**, Mayer, L., Theyer, F., et al., pp. 581–608. Washington: U.S. Government Printing Office 1985

Riedel, W.R., Sanfilippo, A.: Stratigraphy and evolution of tropical Cenozoic radiolarians. Micropaleontology **24,** 61–96, 1978

Ryan, W.B.F., Cita, M.B., Dreyfus-Rauson, M., Burckle, L.H., Saito, T.: A paleomagnetic assignment of Neogene stage boundaries and the development of isochronous datum planes between Mediterranean, the Pacific, and Indian Ocean in order to investigate the response of the world ocean to the Mediterranean "Salinity crisis". Riv. Ital. Paleont. Strat. **80,** 631–688, 1974

Tauxe, L., Tucker, P., Petersen, N.P., LaBrecque, J.L.: Magnetostratigraphy of Leg 73 sediments. In: Initial reports of the Deep Sea Drilling Project, vol. **73**. Hsü, K.J., LaBrecque, J.L., et al., pp. 609–622. Washington: US Government Printing Office 1984

Theyer, F., Hammond, S.R.: Paleomagnetic polarity sequence and radiolarian zones, Brunhes to polarity Epoch 20. Earth Planet. Sci. Lett. **22,** 307–319, 1974

Theyer, F., Mato, C.Y., Hammond, S.R.: Paleomagnetic and geochronologic calibration of latest Oligocene to Pliocene radiolarian events, equatorial Pacific. Marine Micropaleontology **3,** 377–395, 1978

Tracey, J.I., et al.: Initial reports of the Deep Sea Drilling Project **8.** Washington: U.S. Government Printing Office 1971

van Andel, T.H., et al.: Initial reports of the Deep Sea Drilling Project **16.** Washington: U.S. Government Printing Office 1973

van Andel, T.H., Heath, G.R., Moore, T.C.: Cenozoic history and paleo-oceanography of the central equatorial Pacific ocean. Geol. Soc. Am. Mem. **143,** 1–134, 1975

Weinreich, N.: Magnetische Untersuchungen neogener pelagischer Sedimente des zentralen Äquatorialpazifik. Ph.D. thesis, Ruhr-Universität Bochum, 1985

Weinreich, N., Theyer, F.: Paleomagnetism of the Leg 85 sediments: Neogene magnetostratigraphy and tectonic history of the Central Equatorial Pacific. In: Initial reports of the Deep Sea Drilling Project vol. **85**, Mayer, L., Theyer, F., et al., pp. 849–901. Washington: US Government Printing Office 1985

Winterer, E.L.: Sedimentary facies and plate tectonics of the equatorial Pacific. Am. Assoc. Petrol. Geol. Bull. **57,** 265–282, 1973

Zijderveld, J.D.A.: A.C. demagnetization of rocks: analysis of results. In: Methods in palaeomagnetism, Collinson, D.W., Creer, K.M., Runcorn, S.K., (eds.), Amsterdam: Elsevier 1967

Received April 2, 1985 / revised August 22, 1985,
and March 10, 1986
Accepted April 2, 1986